

**VLBI Imaging of Luminous Infrared Galaxies:
AGN Cores in Mrk231, UGC 5101 & NGC 7469** ¹

CAROL J. LONSDALE

*Infrared Processing & Analysis Center
California Institute of Technology 100-22
Pasadena, CA 91125;
cjl@ipac.caltech.edu*

COLIN J. LONSDALE

*MIT Haystack Observatory,
Westford, MA 01886;
cjl@haystack.mit.edu*

HARDING E. SMITH

*Center for Astrophysics & Space Sciences
University of California, San Diego
La Jolla, CA 92093-0424;
hsmith@ucsd.edu*

PHILIP J. DIAMOND

*University of Manchester
Jodrell Bank Observatory
Macclesfield, Cheshire SK11 9DL, United Kingdom;
pdiamond@jb.man.ac.uk*

ABSTRACT

We report 18cm VLBI continuum imaging observations at ~ 5 milliarcsecond resolution for UGC 5101, NGC 7469, and Mrk 231, all part of a sample of Luminous Infrared Galaxies which have been shown to have strong VLBI radio cores in a previous 18cm VLBI survey. Mrk 231, generally considered to be a dust-enshrouded QSO, shares many characteristics with quasars, including a broad, Sy1 optical emission spectrum, optical and radio variability, and broad-absorption-line (BAL) spectrum. NGC 7469 is a classical Sy1 galaxy and UGC 5101 is a liner system.

The radio morphology of these three systems on VLBI scales is AGN-like, with well-defined ridgelines and high-brightness yet spatially resolved components. The structure and flux densities of these VLBI components are not consistent with starburst generated radio supernovae of the type found in Arp 220. On scales of ~ 100 pc, and perhaps beyond, the radio continuum in all three objects appears to be dominated by an AGN, not a starburst. Radio emission on larger scales may well originate, in part or in total, in a less compact circumnuclear star-forming region. This is in contrast to the situation thought to prevail in many LIGs which involves a very compact and dense nuclear starforming region.

By placing a lower limit on the AGN-related radio emission, it is possible to shed light on the relative luminosities of the AGN and starburst in these objects. Using the FIR/radio correlation for starburst-related radio emission, we show that, despite the unambiguous evidence for AGN activity in these systems, the AGN luminosity, although energetically important, may be exceeded by the extended starburst luminosity in all three cases, unless the bolometric luminosity of the entire system has been underestimated. The lower limits on AGN-related radio emission indicate that these AGNs are somewhat over-luminous in the radio compared to radio-quiet PG QSOs, and thus that the AGN radio luminosity cannot be used to estimate the bolometric luminosity of the AGN. However, comparing near- and mid-IR luminosities of the LIGs to PG QSOs we find evidence that a significant fraction of the bolometric luminosity of the AGN in Mrk 231, and to lesser extent UGC 5101, may be radiated away from Earth and thus not detected at any wavelength.

The VLBI structure observed in Mrk 231 allows additional interpretation. Confirming and extending VLBI imaging by Ulvestad, Wrobel & Carilli (1999), our continuum image shows a triple structure, with a core and two lobes, classifying it as a Compact Symmetric Object (CS0). It has been suggested that these sources are young, $\tau \ll 10^6$ yr, with the hot spots representing the working surface of a relativistic jet upon the ambient medium. If the southern (primary) lobe/hot-spot in Mrk 231 is confined by ram pressure, we estimate a lobe advance speed, $v_a \sim 10^{-4}c$, and an age for the jet/compact source, $\tau < 10^6$ yr.

We have also imaged the 1667 MHz OH maser emission in Mrk 231, which is extended on scales of 50–100 milliarcsec (40–80 pc) and probably coincides with the inner region of the disk which is seen in CO emission (Bryant & Scoville 1996) and HI absorption (Carilli, Wrobel & Ulvestad 1998). Among OH megamaser sources studied at high sensitivity with milliarcsecond resolution, Mrk 231 is unique in the stringent upper limits placed upon the flux density of compact OH structures of the type found in Arp 220 and other LIGs. It is possible that

the circumnuclear environment of Mrk 231 has been sufficiently disrupted by the emergent QSO that the cool, dense clouds necessary for such compact masers no longer exist.

Subject headings: galaxies: active — infrared: galaxies — radio continuum: galaxies

1. Introduction

The most luminous galaxies in the Local Universe are Luminous Infrared Galaxies (LIGs) which emit the vast majority of their radiant power in the far-infrared. These are gas-rich systems which are in the late stages of collisions or mergers, and extrapolation from the properties of lower luminosity Starburst galaxies suggests that the LIGs should be active star forming systems (see Sanders & Mirabel 1996 for a review). The LIGs also show many characteristics of AGN and their luminosities reach values comparable to those of luminous QSOs. Much effort has been focused on whether the power from the LIGs is principally from starburst or AGN activity, although both types of activity may be present, frequently in the same system. The discussion has been framed around a scenario proposed by Sanders *et al.* (1988) in which a merger of gas-rich disk galaxies stimulates a massive nuclear starburst, which in turn feeds a coalescing AGN core in the galaxy nucleus. As the AGN turns on, radiation pressure drives out the shroud of dust, revealing a nascent quasar. Other authors (Perry & Dyson 1985; Scoville & Norman 1989; Terlevich & Melnick 1985) have proposed variations on the theme of compact, luminous starbursts giving rise to AGN activity. The goal must be not only to understand the dominant source of energy in LIGs, but to understand the relationship between starburst and AGN activity, and other galaxy characteristics, and to place them into an evolutionary context. We have for some time been approaching this problem by investigating the characteristics of a complete sample of LIGs defined by Condon *et al.* (1991; CHYT); this work has concentrated on VLBI observations which offer unique AGN/starburst diagnostics in one of the few wavelength regimes where the optical depths to the active regions may fall below unity.

In a non-imaging 18-cm VLBI survey of Luminous Infrared Galaxies from the CHYT sample for compact, high-brightness temperature emission commonly associated with AGN

¹Based on observations from the VLBA of the National Radio Astronomy Observatory which is a facility of the US National Science Foundation operated under cooperative agreement by Associated Universities, Inc.

activity, Lonsdale, Smith, and Lonsdale (1993; Paper I) showed that milli-arcsecond scale emission with $T_b \gg 10^7 K$ is common, perhaps universal in LIGs. Furthermore, the LIGs follow a similar relationship between core radio power and bolometric luminosity to radio-quiet QSOs (Lonsdale, Smith & Lonsdale 1995). This work lends support to the interpretation of LIGs as dust-enshrouded AGN. On the other hand, in a detailed analysis of our VLBI survey data, Smith, Lonsdale and Lonsdale (1998; Paper II) investigated a Starburst origin for LIGs in which the compact, high- T_b emission is produced by luminous radio supernovae (RSN). This analysis indicates that most, but not all, LIG VLBI-scale emission may be modelled with Starburst-generated RSN, provided the RSN are *extremely luminous*. The predictions of this analysis were confirmed with the detection of luminous RSN in the nuclei of Arp 220, consistent with a Starburst origin for the infrared luminosity of this LIG (Smith *et al.* 1998a). We are continuing a monitoring program of the Arp 220 LRSN allowing refinement of the characteristics of LRSN in the extreme LIG environment; preliminary results (Lonsdale *et al.* 2001) suggest that decay timescales are longer than for “normal” LRSN with a concomitant reduction in our estimate of the rate of luminous RSN — but not total RSN — frequency. Other radio supernova candidates have since been suggested in galaxies studied here — 4 near the nucleus of Mrk 231 (Taylor *et al.* 1999) and 1 in the starburst ring around the nucleus of NGC 7469 (Colina *et al.* 2001).

In this paper we present 18cm VLBI imaging of Mrk 231, UGC 5101 and NGC 7469, LIGs which had VLBI detections in our survey of a character which cannot be adequately fitted by multiple, luminous radio supernovae — either isolated or in clumps. All three galaxies have also commonly been interpreted as AGN based on optical spectroscopic data. These continuum imaging observations are designed to determine the nature of the central radio cores in Mrk 231, UGC 5101, and NGC 7469, to investigate the relationship between AGN and starburst within these 3 LIGs, and to investigate the relationship between these galaxies and other AGN and LIG systems. We also present 18cm imaging observations of Mrk 231 in the 1667MHz OH maser line.

1.1. UGC 5101

UGC 5101 ($D = 164\text{Mpc}$; $1'' \sim 800\text{pc}$) is a liner system with a strongly interacting morphology (Sanders *et al.* 1988). A weak soft Xray detection by ROSAT has been reported by Rigopoulou, Lawrence & Rowan-Robinson (1996). UGC 5101 has an estimated reservoir of molecular gas, $\log M_{H_2} = 10.3M_\odot$ (Solomon *et al.* 1997) and a FIR luminosity, $\log L_{FIR} = 11.96L_\odot$ (Sanders *et al.* 2003). With a VLBI flux density estimated from our survey observations, $S_{vlbi} \approx 28\text{mJy}$, nearly 20% of the 18cm flux density was seen in the

compact core; this is the highest ratio of core-to-total flux density among the 40 LIGs in our complete sample.

Soifer *et al.* (2000) have presented mid-infrared (MIR) imaging of UGC 5101 using MIRLIN at Keck and have compared it to IRAS fluxes. They find a compact unresolved core of extent less than $0''.22$ (~ 175 pc) at $12.5\mu\text{m}$, surrounded by more diffuse emission on scales of $\sim 1''$. About 60% of the entire $12\mu\text{m}$ flux measured in the large IRAS beam is contained within in their $4''$ measurement, and 30% of the entire $12\mu\text{m}$ flux is within the unresolved core. At $17.9\mu\text{m}$ the structure is consistent with that at $12.5\mu\text{m}$.

Scoville *et al.* (2000) have obtained near-infrared (NIR) HST/NICMOS images of UGC 5101 with resolution about $0''.2$. The nuclear source in the near-infrared image is better fit with an $r^{1/4}$ law than an exponential, with $R_{1/2} < 0.5\text{kpc}$. Scoville *et al.* conclude that although it is a cool far-infrared source, UGC 5101 has nuclear NIR colors more similar to those of warm ULIRGs; specifically redder in $[m_{1.6} - m_{2.2}]$ than in $[m_{1.1} - m_{1.6}]$ than other cool ULIRGs. They deduce that a visual extinction of $A_v \gg 50$ mag is required to explain such colors by a starburst model in which the gas is mixed with the dust. The near-infrared colors are alternatively consistent with a central AGN with high extinction, or a much less extinguished AGN plus warm dust emission at $2.2\mu\text{m}$.

Soifer *et al.* (2000) compare their $12\mu\text{m}$ image with the NICMOS NIR image of Scoville *et al.* (2000) and the VLA 8.4GHz image of CHYT, finding the sources aligned at these three frequencies, insofar as the relative astrometry allows.

Tran *et al.* (2001) have analysed the $3'$ aperture ISO CVF observations of the MIR spectrum of UGC 5101 in terms of a starburst and an AGN contribution, based on the ratio of the strength of the $7.7\mu\text{m}$ unidentified feature relative to the continuum, combined with the $5\text{--}10\mu\text{m}$ continuum colors. They conclude that approximately 50% of the MIR continuum could come from an AGN, which is consistent with the result of Soifer *et al.* that $\sim 30\%$ of the the total IRAS $12\mu\text{m}$ flux comes from the unresolved ($< 0''.22$) MIR core.

Spoon *et al.* (2002) report detection of the $6.0\mu\text{m}$ water ice feature in ISO-PHT-S spectroscopy of UGC 5101, the strongest amongst the 20 galaxies in their sample, as well as strong $9.7\mu\text{m}$ silicate absorption and PAH emission features. Within the large ISO beam it is not possible to determine the scale on which the absorption is occurring. They caution that the detailed structure of the absorption features and MIR continuum complicates the attempt to separate the starburst vs AGN contributions to the luminosity by Tran *et al.* . Also, the presence of the deep silicate feature may affect Soifer *et al.*'s conclusion that only 30% of the total IRAS flux arises from the unresolved core. Moreover, both the Tran *et al.* and Soifer *et al.* studies could have underestimated the total MIR radiation arising from the

AGN if the extinction to the nucleus is significant in the MIR.

1.2. NGC 7469

NGC 7469 ($D = 66$ Mpc) is a classical Seyfert Galaxy (Seyfert 1943) which has subsequently been classified as a Sy1–1.2 galaxy based on the strengths of the broad and narrow components of its optical emission lines. NGC 7469 is strongly interacting with a nearby companion, IC5283 (Dahari 1985). The galaxy shows a strongly variable UV/optical continuum with low extinction, and X-ray emission which is variable on time-scales of ~ 1 day (Nandra *et al.* 2000) with a complex iron line spectrum from BeppoSAX (De Rosa, Fabian & Piro 2002). There is evidence for an $\sim 10^7 M_{\odot}$ central black hole from reverberation mapping (Peterson & Wandel 2000). NGC 7469 shows nuclear non-thermal radio emission as expected for classical AGN, but also shows a dual ring of star formation 1–3'' and 8–10'' from the nucleus. The inner starburst ring is detected at radio (Wilson *et al.* 1991), mid-infrared (Miles, Houck & Hayward 1994; Smith *et al.* 1998b; Soifer *et al.* 2003) and optical wavelengths (Mauder *et al.* 1994).

About half of the $12\mu\text{m}$ emission originates in this starburst ring, which also shows the $11.3\mu\text{m}$ emission feature commonly associated with regions of strong star formation, but the ratio of nuclear ring emission increases at longer wavelengths, suggesting that the nucleus may dominate in the FIR (Smith *et al.* 1998b). NICMOS observations of NGC 7469 by Scoville *et al.* reveal that $>30\%$ of the $2.2\mu\text{m}$ flux from the galaxy arises within a radius of $0''.12$, or $\lesssim 77\text{pc}$. Alonso-Herrero *et al.* (2001) determine non-stellar nuclear fluxes for NGC 7469 between $1\text{--}5\mu\text{m}$, which together with ISO fluxes they model in terms of a close to face-on dusty molecular torus.

The system is gas-rich with $M_{H_2} = 10^{10} M_{\odot}$ (Sanders, Scoville & Soifer 1991). Our VLBI survey observations (Lonsdale, Smith & Lonsdale 1993) showed a strong compact radio core with an estimated flux density of 12mJy, about 6% of the integrated 18cm radio emission, and an estimated brightness temperature in excess of 10^7K . MERLIN observations at 18cm by Thean *et al.* (2001) show a barely resolved nuclear source with ~ 30 mJy, surrounded by more diffuse emission associated with the inner starburst ring. This result implies that our VLBI survey observations were insensitive to 15–20 mJy of emission on scales $\lesssim 0.1$ arcsec. A careful registration of the new $11.7\mu\text{m}$ image of NGC 7469 of Soifer *et al.* (2003) with the archived MERLIN 18cm map of Thean *et al.* (2001) indicates that the compact radio and mid-infrared cores align to better than $\sim 80\text{mas}$; see Soifer *et al.* (2003).

1.3. Mrk 231

Mrk 231 (=UGC 5058; $D = 173$ Mpc; $1'' = 840$ pc for $H_0 = 75\text{km s}^{-1}\text{Mpc}^{-1}$) has long been recognized as a remarkable galaxy: it is the most luminous galaxy in the local ($z \lesssim 0.1$) Universe with characteristics that place it among classical AGN (Boksenberg *et al.* 1977) and also infrared galaxies (Sanders *et al.* 1988). Our interest in Mrk 231 was stimulated by the 1993 18cm VLBI survey (Lonsdale, Smith & Lonsdale 1993) which demonstrated that Mrk 231 has a strong, high-brightness temperature, VLBI core radio source which accounts for a major fraction of its 18cm radio emission. In its radio properties Mrk 231 is thus the most “quasar-like” of our VLBI sample and of the complete sample of Luminous Infrared Galaxies (Condon *et al.* 1991) from which our sample was derived.

1.3.1. Mrk 231 as a QSO

Mrk 231 has long been considered an infrared quasar — the integrated luminosity of Mrk 231, $L_{bol} \gtrsim 10^{46} \text{erg s}^{-1}$, is comparable to other low-redshift ($z \lesssim 1$) radio-quiet QSOs and it falls in the midst of the radio power-luminosity relation for QSOs (and LIGs) constructed by Lonsdale, Smith & Lonsdale (1995). Mrk 231 is reported to be variable at optical (Hamilton & Keel 1987), radio (McCutcheon & Gregory 1978), and X-ray wavelengths (Gallagher *et al.* 2002).

The core of Mrk 231 has been imaged by HST at $1.6\mu\text{m}$ (Quillen *et al.* 2001), revealing an unresolved point source, $\text{FWHM} \lesssim 0.13''$ (109pc) with absolute magnitude $M_H \sim -26$, which is comparable to the most luminous $z < 0.2$ PG QSOs. Adaptive optics imaging by Lai *et al.* (1998) detected a point source of $\text{FWHM} 0.1''$, with $[J - H] = 0.99$, $[H - K] = 1.12$. Mrk 231 shows a strong, broad optical type 1 emission-line spectrum with strong FeII emission. The optical lines and continuum are reddened with $A_V \approx 2$ (Boksenberg *et al.* 1977; Lipari, Colina & Macheto 1994), and the optical/NIR continuum polarization level decreases from as high as 20% in the UV towards longer wavelengths (Smith *et al.* 1995), interpreted as a complex scattering geometry in which most lines of sight to the nucleus are moderately obscured.

Mrk 231 was imaged at Keck in 7 MIR bands from 7.9 to $19.7\mu\text{m}$ by Soifer *et al.* (2000), and found to be unresolved at $0.13''$ in all bands; *i.e.* on a similar 100pc scale as the NIR point source. All of the $12\mu\text{m}$ IRAS emission in a much bigger beam is contained within this unresolved source. Spoon *et al.* (2002) have recently published an ISO-PHT-S MIR spectrum of Mrk 231, which shows strong silicate $9.7\mu\text{m}$ absorption, and probably water ice $6.0\mu\text{m}$ absorption, interpreted as a molecular torus around the AGN. The extinction to

the AGN cannot be directly estimated from the depth of the silicate absorption because it depends strongly upon viewing angle, involving radiative transfer through the few pc-diameter torus (Efsthathiou & Rowan-Robinson 1995).

Mrk 231 is a low-ionization BAL (Broad Absorption Line) object with three systems: $v_{ej} \approx 4700 \text{ km/s}$, $v_{ej} \approx 6000 \text{ km/s}$, $v_{ej} \approx 8000 \text{ km/s}$ (Adams & Weedman 1972; Boksenberg *et al.* 1977; Rudy, Foltz & Stocke 1985). The $v_{ej} \approx 8000 \text{ km/s}$ absorption-line system is variable on timescales of order 2–3 yrs (Boroson *et al.* 1991; Forster, Rich & McCarthy 1995). Mrk 231 is underluminous in x-rays between 0.1–10keV (Maloney & Reynolds 2000; Gallagher *et al.* 2002) and soft γ -rays (Dermer *et al.* 1997) a characteristic it shares with other BAL objects (Gallagher *et al.* 1999). Spectroscopy with Chandra (Gallagher *et al.* 2002) in the 2–10keV range reveals a hard spectrum, interpreted as several scattered emission components, and rapid variability which ties the emission to within light-hours of the central black hole. Neither Chandra nor ASCA (Maloney & Reynolds 2000) directly detects a hard X-ray power-law, indicating the presence of a Compton-thick absorber, $N_H > 10^{24}$. Gallagher *et al.* (2002) suggest the absorber could be the so-called “hitchhiking” gas at very small radii ($\sim 10^{15}$ cm), invoked to protect the BAL wind from ionization by the UV and soft-X-ray photons (Murray *et al.* 1995). The X-ray absorber must be small to avoid blocking the highly variable light-hour-scale scattered X-ray component from view.

1.3.2. Mrk 231 as a Luminous Infrared Galaxy

With an infrared luminosity, $\log L_{FIR} = 12.51L_\odot$ (Sanders *et al.* 2003), Mrk 231 is the most luminous infrared galaxy in the complete sample of 40 LIGs of CHYT from the IRAS Bright Galaxy Sample. Like Arp 220 and other well-studied LIGs, the system is rich in molecular gas, $\log M_{H_2} \approx 10.2M_\odot$ (Scoville, Yun & Bryant 1997) and it is one of the original OH megamaser systems (Baan 1985). Furthermore, Mrk 231 shows tidal tails and other evidence for merger or disturbance in the “host” galaxy, which is itself a luminous system with evidence for rapid star formation (Hamilton & Keel 1987; Sanders *et al.* 1988).

The CO in Mrk 231 has been studied at high resolution by Bryant & Scoville (1996) who show that the CO distribution is elongated with a velocity gradient aligned with the major axis of the CO distribution. They interpret the CO distribution as a disk, oriented roughly E–W, containing an estimated $3 \times 10^9 M_\odot$ of molecular gas within a diameter of about $1'' (=840 \text{ pc})$ and a scale height, $h \approx 30 \text{ pc}$. Bryant & Scoville find the CO brightness temperature to be comparable to the FIR dust temperature, $T_b(CO) \sim T_{fir} \sim 85 \text{ K}$ and suggest that the disk is filled with dense gas clouds, which may account for the accretion rate required to power the luminous nucleus.

In a comprehensive series of papers Ulvestad and colleagues have described results from a multi-frequency set of VLBA/VLA observations of Mrk 231. Ulvestad, Wrobel & Carilli (1999) present observations from 1.4–15GHz which show a central north-south triple source with overall extent $\lesssim 100\text{mas}$ (80pc), indicative of an AGN in structure. Both lobes of the north-south triple show evidence for free-free absorption near 2 GHz which is interpreted as due to ionized gas with $n_e \sim 10^3\text{cm}^{-3}$. The central (nuclear) component of the triple shows resolution above 5GHz and is resolved into 2 or possibly 3 components at 15GHz with extent $\sim 3\text{mas}$ (2pc) at PA 65° .

21cm line continuum observations with the VLBA (Carilli, Wrobel & Ulvestad 1998) show emission from an extended “disk” with a size of 440mas (370pc) which exhibits HI *absorption* against radio emission from the inner disk ($r \lesssim 160\text{pc}$), but not against the central radio core. The HI observations suggest $N_{\text{HI}} \approx 6 \times 10^{22} (T_s/1000\text{K}) \text{cm}^{-2}$; $\langle n_{\text{HI}} \rangle \approx 250 (T_s/1000\text{K}) \text{cm}^{-3}$; and $M_{\text{HI}} \approx 2 \times 10^7 (T_s/1000) M_\odot$, where T_s is the spin temperature. These observations are consistent with the neutral hydrogen lying in a disk structure of sub-kpc dimension. Further continuum observations reported by Taylor *et al.* (1999) trace this emission out to nearly $1''$. They interpret the disk radio emission as due to star-formation activity, $\dot{m} \sim 60 - 220 M_\odot \text{yr}^{-1}$.

On larger scales Ulvestad, Wrobel & Carilli (1999) find continuum emission emerging from the core near star-forming knots (Surace *et al.* 1998), extending to the south for about $20''$, coincident with regions of H α emission (Hamilton & Keel 1987), then curving toward the west in the general detection of the tidal tails observed by Hamilton & Keel (1987) and Surace *et al.* (1998). They interpret this kpc-scale radio emission as nonthermal emission powered by a jet from the nucleus, principally due to the high degree of linear polarization and the highly ordered magnetic field implied. This emission has previously been interpreted as due to a starburst-driven superwind by Baum *et al.* (1993).

2. VLBI Observations

Observations of UGC 5101 and NGC 7469 were obtained as part of VLBA continuum imaging experiment BL6 on 16 January 1995. All 10 telescopes of the VLBA were used, with on-source integration times of roughly 4 hours per source. UGC 5101 and, in particular, NGC 7469 are relatively weak sources on VLBI scales, as are most of the LIGs in our original VLBI Survey sample, so conventional self-calibration and hybrid mapping techniques were not readily applicable.

However, unrelated compact radio sources bright enough for VLBI fringe-fitting lie

within a few arcminutes of both galaxies, and it was possible to perform in-beam phase referencing to calibrate the phases of the target sources. In fact, UGC 5101 and NGC 7469 were selected for this imaging program as having nearby calibrators within the 30' primary beam from a survey of our original list of LIGs with compact VLBI-scale radio emission. The phase solutions from SELFCAL show a point-to-point scatter smaller than 10° , commensurate with the signal-to-noise ratio of about 5 for these solutions, and these solutions appear adequate for well over 95% of the data. Long-term trends in phase consistent with typical L-band atmospheric/ionospheric drifts are evident and benign. In this way we were able to produce accurate maps with peak flux densities as low as 1.4 mJy. Typical background rms levels of $60\mu\text{Jy}$ for NGC 7469 and $80\mu\text{Jy}$ for UGC 5101 were achieved.

Table 1. Calibrators for VLBI Experiment BL6

VLBI Source	Calibrator	α	δ	RA Offset	Dec Offset	$S_{1.67}^{pk}$ (mJy)
(1)	(2)	(3)	(4)	(5)	(6)	(7)
UGC 5101	0935+6117	09 ^h 35 ^m 30 ^s .865	+61° 17' 24".129	2' 31"	3' 48"	34
NGC 7469	2303+0850	23 ^h 03 ^m 11 ^s .912	+08° 50' 13".029	0' 54"	2' 13"	7

Emission was detected on a variety of size scales, particularly in UGC 5101. The surface brightness sensitivity of the images is a strong function of the data weighting during the mapping process, so we present two images of UGC 5101, one optimizing angular resolution for the purpose of estimating the sizes of compact features, and one with lower resolution, but a better representation of diffuse emission.

The observations of Mrk 231, conducted under project code GL15 on 13 November 1994, involving 17 telescopes in Europe and the U.S., were designed to provide full imaging in line and continuum for the four brightest OH megamaser sources in the northern sky, including III Zw 35, Mrk 231, Arp 220 and IRAS17208–0014. Mrk 231 received a long track, of which ~ 4 hours was spent on-source, yielding excellent u – v coverage. After correlation in April 1996, standard hybrid mapping techniques were used to reduce the observations of this relatively bright source. The rms noise levels achieved were close to $60\mu\text{Jy}/\text{beam}$. As for UGC 5101, we show two images, one optimized for angular resolution, and the other to better delineate more extended emission.

Our VLBI maps of the three galaxies are shown in Figures 1–3: Figure 1 shows UGC 5101; (1a) is a near-uniform weighting map exhibiting the highest resolution (with gaussian restoring beam $7.6\times 6.2\text{mas}$ in PA 24° and (1b) is a map tapered to display extended emission (convolution size $11.6\times 9.9\text{mas}$ in PA 42°). Figure 2 shows the map of NGC 7469 (convolution size $13.7\times 7.9\text{mas}$ in PA -8°). Figure 3 shows Mrk 231; (3a) is the uniformly weighted image with a 4.8×3.4 milliarcsec beam, and (3b) is the naturally weighted image with a 6.1×4.2 milliarcsec beam.

3. Results

3.1. UGC 5101

The image of UGC 5101 (Figure 1) displays three major compact, high brightness temperature components in the NW, and a more diffuse component in the SE. The compact components are barely resolved, implying diameters $\lesssim 3 - 4\text{pc}$. There is faint diffuse emission connecting the 3 compact components, which lie within an area of $\sim 60\times 30\text{mas}$ (RA \times Dec), or $48\times 24\text{pc}$. The SE diffuse component, A, lies about 60 pc from the easternmost compact component, and a wisp of diffuse emission extends from it towards the compact components. Component A is clearly associated with a spur of emission visible on the highest resolution VLA images of SLL98 on $0''.1$ scales. It is likely that the flux density of this diffuse structure has been significantly underestimated by our VLBI observations. Details for the compact components are given in Table 2: column (1) gives our component designation; columns

(2) and (3) the positional offset from component “C”; column (4) the peak 1.67GHz flux density; column (5) the integrated 1.67GHz flux density; columns (6), (7), (8) the major and minor axial extent and the position angle of an elliptical gaussian fit from AIPS procedure JMFIT and column (9) the integrated radio luminosity (10MHz–100GHz) from standard synchrotron theory (Conway *et al.* 1983).

The major components lie along a discernible ridge line; at the three compact components the ridge line is at approximate position angle 107° , then it bends to $\sim 135^\circ$ towards the diffuse component. The total extent of the VLBI-scale structure is $0''.13 \times 0''.12$ (RA \times Dec), which corresponds to 103×95 pc at the distance of 164 Mpc adopted for UGC 5101. Our experiment is not sensitive to diffuse extended structures on scales significantly larger than these. The total flux detected in our experiment is 38 mJy, which is over 25% of the 18 cm emission detected on scales of $1''.5$ with the VLA (Condon *et al.* 1991).

The fact that the major components form a rough ridge-line, coupled with the evidence for diffuse emission connecting the components, strongly suggests an AGN-generated jet structure. If this is the correct interpretation for these features, one of the compact sources is likely to be the core and the others to be knots in the jet. We cannot tell from our single frequency data which of the compact components is likely to be the core. The diffuse component may be due to strong interaction between the jet and surrounding ISM, decollimating and bending the flow. There is no evidence for any bow shock or limb brightening in the diffuse component. The appearance is reminiscent of centrally-peaked Fanaroff and Riley type I morphology associated with low-luminosity extragalactic radio sources.

The general appearance of the UGC 5101 VLBI structures resembles compact jets in other AGN observed with 18cm VLBI — *e.g.* 0402+379=4C37.11, 0831+557=4C55.16, 0900+428=4C42.28, *etc.*, in the Caltech Jodrell Bank VLBI Survey (Politidis *et al.* 1995).

It is very unlikely that the compact structures in UGC 5101 are radio supernovae, (RSN) such as those we discovered in Arp 220 (Smith *et al.* 1998a). The individual UGC 5101 components are up to ~ 30 times more luminous than the brightest Arp 220 RSN. Moreover evidence for extension of the compact components indicates source sizes much too large for a single RSN, which expand at a rate of about 0.01 pc yr^{-1} ($0.013 \text{ mas yr}^{-1}$) near maximum, corresponding to minimum ages exceeding 300yr for resolved features. Neither can clusters of RSN straightforwardly explain the compact emission: the RSN rate implied by the FIR luminosity of UGC 5101 is $\nu_{sn} \approx 1 \text{ yr}^{-1}$ comparable to that for Arp220 (Smith, Lonsdale & Lonsdale 1998), but the components A–D are each factors of several greater in radio power than the total 1.67GHz radio power of the Arp220 RSN (Smith *et al.* 1998a).

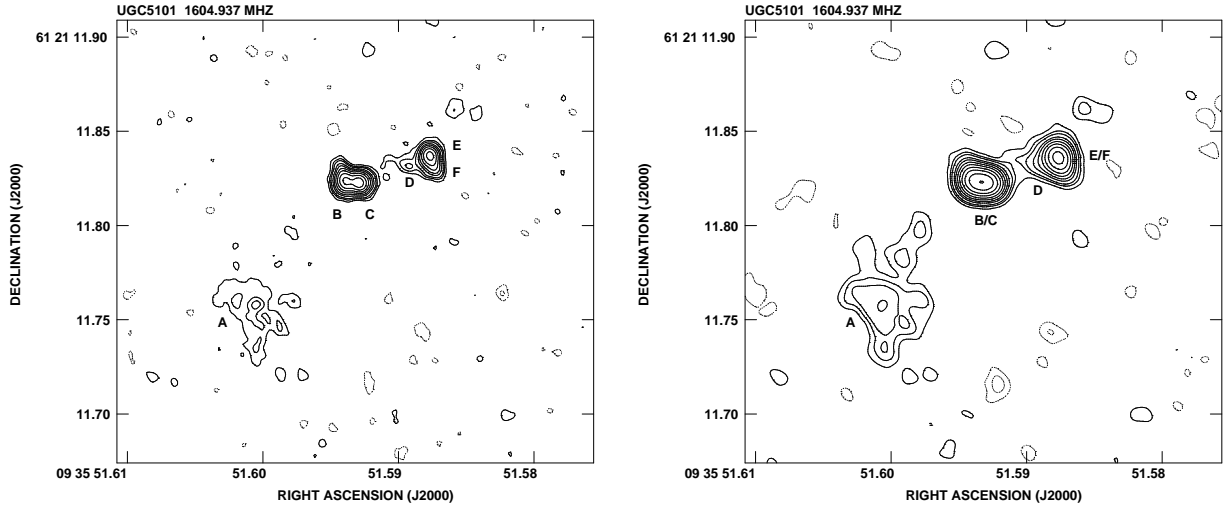


Fig. 1.— VLBI continuum images of UGC 5101. (1a) is a near-uniform weighting map exhibiting the highest resolution (with gaussian restoring beam 7.6×6.2 mas in PA 24° ; (1b) is a map tapered to display extended emission (convolution size 11.6×9.9 mas in PA 42°). Contours are -0.6, -0.4, -0.2, 0.2, 0.4, 0.6, 1.0, 1.4, 2.0, 2.8, 4.0, 5.6, 8.0, 11.2 mJy.

Table 2. COMPACT 18cm COMPONENTS IN UGC 5101

Component	$\Delta\alpha$ (mas)	$\Delta\delta$ (mas)	$S_{1.67}^{pk}$ (mJy)	$S_{1.67}^{int}$ mJy	θ_{maj} (mas)	θ_{min} (mas)	p.a. ($^{\circ}$)	L_{radio} ($erg\ s^{-1}$)
(1)	(2)	(3)	(4)	(5)	(6)	(7)	(8)	(9)
$S_{vlbi} = 38\text{mJy}$								
A	~ 55	~ -65	...	9.6 ± 0.7	5.4×10^{39}
B	8.1	1.2	5.2 ± 0.1	8.2 ± 0.5	< 8	< 8	177:	4.7×10^{39}
C	0	0	6.8 ± 0.1	10.4 ± 0.5	6 ± 1	< 5	104 ± 40	6.2×10^{39}
D	~ 25	~ 10	...	0.8 ± 0.1
E	37.7	15.2	3.8 ± 0.1	4.5 ± 1.0	< 6	< 6	...	2.6×10^{39}
F	38.3	9.2	2.2 ± 0.1	4.5 ± 1.0	< 10	< 10	54 ± 5	2.4×10^{39}

The upper limit to the size of the mid-infrared core source detected by Soifer *et al.* (2000) — $\lesssim 175$ pc — is comparable to the total size of our 18 cm source, and is coincident with it within the positional uncertainty of the mid-infrared image.

3.2. NGC 7469

The image of NGC 7469 displays 5 compact sources which lie roughly on an E–W line. The 2 western sources are well resolved, and the westernmost could itself be double. Two of the 3 eastern sources are unresolved, and the central of these three has marginal evidence for resolution. There is one additional possible source to the south at low SNR, with flux about 0.3 mJy. See Table 3 for details; column legend is as for Table 2.

There is no VLBI evidence for diffuse emission, connecting ridges or jets between the compact sources. The source complex is contained within an area of dimension ~ 168 mas (~ 54 pc) EW. Diffuse emission on scales greater than about $0''.1$ (~ 30 pc) would not have been detected by our experiment. However, the total flux density detected in our experiment is about 15 mJy, which is $\sim 50\%$ of the flux density seen by Thean *et al.* (2001) within a $\sim 0''.15$ nuclear component at 18cm using MERLIN. Their contour map indicates clear evidence for E–W extension of the nuclear component with a size and orientation consistent with our VLBI-scale structure. The MERLIN data indicate that our VLBI components are embedded in a region of somewhat more diffuse emission with a scale of order 150 mas (48 pc), which was resolved out on the VLBI baselines. The small size of the MERLIN component implies that the compact and diffuse components of the structure are coincident on the sky (*i.e.* the compact VLBI components are embedded within the diffuse emission). Furthermore, the “diffuse” MERLIN component is itself compact by the standards of starburst-related diffuse emission, with a brightness temperature approaching 10^6 K, and is thus not readily associated with star-formation as opposed to an AGN-related radio source.

The unresolved sources could in principle be individual RSN like those in Arp 220 (Smith *et al.* 1998a), being up to a factor of two more luminous than the Arp 220 RSN; the resolved western features, which are too large to be individual RSN (see Table 2), could be clumps of luminous RSN. We consider this unlikely for several reasons: 1) the inferred supernova rate in NGC 7469, ascribing *all* infrared emission to a Starburst origin, is about a factor of 5 lower than for Arp 220 (Smith, Lonsdale & Lonsdale 1998), 2) reasonable combinations of supernova luminosity and age would require some resolution of such a clump of RSN, and 3) one would expect compact AGN emission coincident with the Sy 1 nucleus whereas RSN would be expected to be found in the Starburst ring. The most plausible hypothesis, which we adopt, is that the small-scale nuclear radio emission in NGC 7469 is AGN-related.

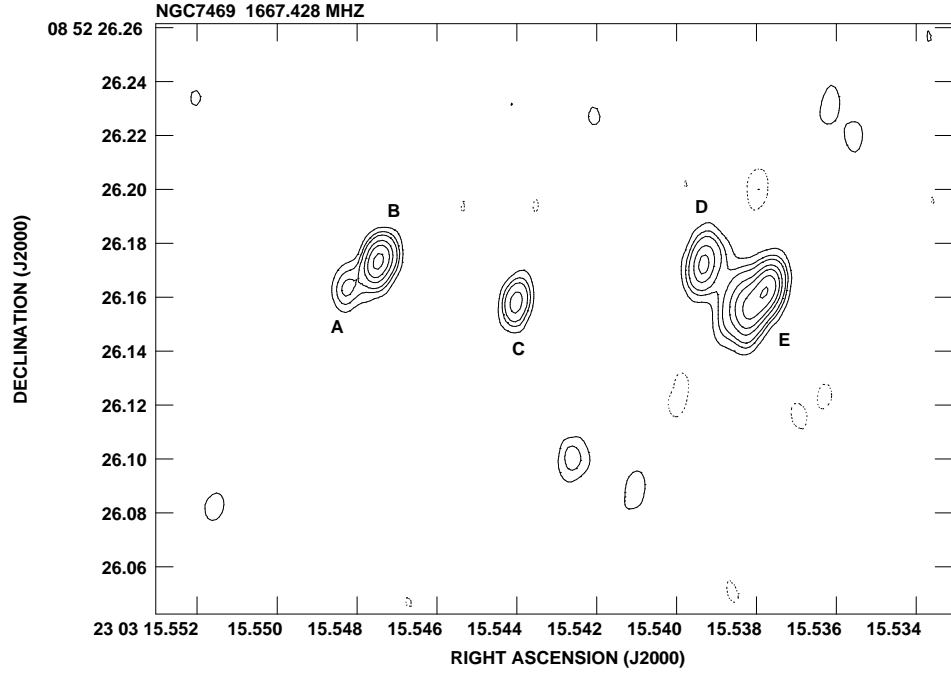


Fig. 2.— 1.67MHz near-uniform weighting map of NGC 7469 (convolution size 13.7×7.9 mas in PA -8°). Tapering reveals no further extended emission. Contours are -0.3, -0.2, -0.1, 0.1, 0.2, 0.3, 0.5, 0.7, 1.0, 1.4mJy.

Table 3. COMPACT 18cm COMPONENTS IN NGC 7469

Component	$\Delta\alpha$ (mas)	$\Delta\delta$ (mas)	$S_{1.67}^{pk}$ (mJy)	$S_{1.67}^{int}$ mJy	θ_{maj} (mas)	θ_{min} (mas)	p.a. ($^{\circ}$)	L_{radio} ($erg\ s^{-1}$)
(1)	(2)	(3)	(4)	(5)	(6)	(7)	(8)	(9)
$S_{vlbi} = 14.8\text{mJy}$								
A	54.2	6.3	0.7 ± 0.1	1.4 ± 0.2	< 19	< 19	...	1.3×10^{38}
B	51.2	15.2	2.1 ± 0.1	2.7 ± 0.2	< 8	< 8	...	2.5×10^{38}
C	0	0	1.2 ± 0.1	1.2 ± 0.1	< 5	< 5	...	1.1×10^{38}
D	-69.8	14.1	1.3 ± 0.1	2.8 ± 0.2	13 ± 1	8 ± 1	16 ± 6	2.5×10^{38}
E	-89.7	1.5	2.6 ± 0.1	7.4 ± 0.3	21 ± 1	7 ± 1	135 ± 5	6.9×10^{38}

The Scoville *et al.* NICMOS images of NGC 7469 have a limit on the core size $\lesssim 77\text{pc}$ which is comparable to the overall dimension of the structures detected in our images: $\sim 54\text{pc}$. The $12\mu\text{m}$ core is similarly self-consistent in size to the VLBI image, and is coincident with it to $\sim 40\text{mas}$ (13pc) (Soifer *et al.* 2003).

3.3. Mrk 231

Our global VLBI experiment exhibits better resolution and somewhat lower noise than the 1.4GHz VLBA image of Ulvestad, Wrobel & Carilli (1999), but generally confirms their results. The central 100mas exhibits a compact core with roughly symmetrically placed lobes approximately 30mas north and south. The southern lobe exhibits strong brightening at the extreme limb, which almost certainly represents the bow shock at the working surface of a nuclear jet upon the ambient medium.

3.3.1. *The Compact AGN Continuum Source in Mrk 231*

The radio morphology of the central region of Mrk 231 ($\theta \lesssim 0''.1$, $d \lesssim 84\text{pc}$) places it among the “Compact Symmetric Objects” — CSOs (Wilkinson *et al.* 1994) — in which radio emission originates from hot spots or lobes symmetrically placed on sub-kpc scales about a central compact source. Readhead *et al.* (1996) list a dozen characteristics which are exhibited by all or some of the 5 confirmed CSOs in the Pearson & Readhead (1988) and Caltech-Jodrell Bank (Politidis *et al.* 1995; Henstock *et al.* 1995) VLBI samples, including high-luminosity, variability, optical evidence for interaction (in one case), etc. Mrk 231 shares most of these characteristics with the exception that in Mrk 231 the core fraction is much higher than in the confirmed CSOs and that other CSOs appear to be in E galaxies dominated by an old stellar population, whereas Mrk 231 is a gas-rich system with a strong starburst. Also, by the above definition a common characteristic of CSOs is lack of extended emission on scales larger than 1 kpc, whereas Mrk 231 shows extended emission due perhaps to a superwind from the circumnuclear starburst (Ulvestad, Wrobel & Carilli 1999).

It has been suggested that the CSOs are young, $\tau \ll 10^6\text{yr}$, with the hot spots representing the working surface of a relativistic jet upon the ambient medium. In this picture the hot spots are confined by ram pressure, advancing with inferred typical speed, $v_a \sim 0.02c$ (Readhead *et al.* 1996); advance speeds measured by Taylor *et al.* (2000) for 4 CSOs are an order of magnitude larger, of the order of $0.1\text{--}0.5h^{-1}c$, with kinematic ages ranging from 300 – 1200 yr.

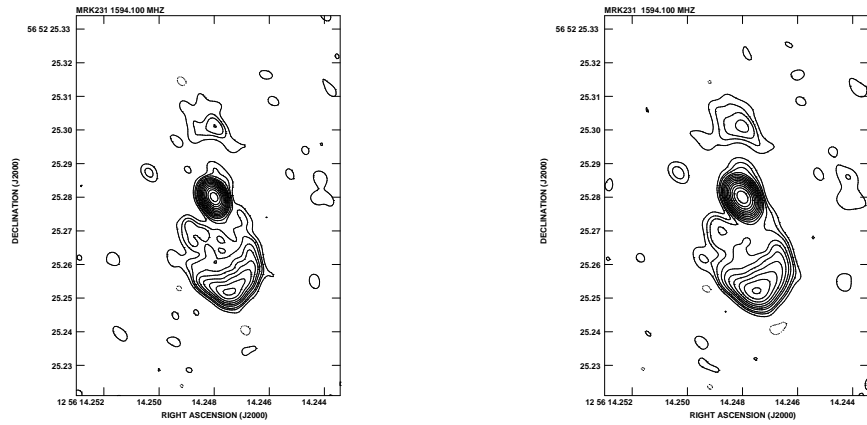


Fig. 3.— VLBI continuum images of Mrk 231. (3a) is the uniformly weighted image with a 4.8×3.4 milliarcsec beam; (3b) is the naturally weighted image with a 6.1×4.2 milliarcsec beam. Contours are -0.6, -0.4, -0.2, 0.2, 0.4, 0.6, 1.0, 1.4, 2.0, 2.8, 4.0, 5.6, 8.0, 11.2, 16.0, 22.4, 32.0 mJy

Table 4. Mrk 231 RADIO COMPONENTS

Component	Scale		$S_{1.6GHz}$ (mJy)	Reference
(1)	(2)	(3)	(4)	(5)
Extended	$> 1''$	Superwind?	42	Ulvestad, Wrobel & Carilli (1999)
	$0''.1 - 1''.0$	Starburst/Molecular Disk	130	Carilli, Wrobel & Ulvestad (1998)
Core	$< 0''.005$	AGN Core	43 ± 4	This work
South Lobe		Jet Interaction Region	44 ± 6	This work
North Lobe		Jet Interaction Region	4 ± 1	This work

As for UGC 5101 and NGC 7469, the limits on the compact NIR and MIR $12\mu\text{m}$ core is found to be of similar scale — $\lesssim 100\text{pc}$ — to the VLBI structures.

We focus on the Southern Lobe/Interaction Region in order to estimate the age of the radio source and, by implication, that of the QSO core. We have used standard synchrotron theory, assuming equipartition between particle and field energy (minimum energy), to model the physical characteristics of the south lobe, which we assume to be the interaction region between a sub-relativistic jet and ambient gas:

- Total Energy: $U_{Tot} \sim 10^{52}\text{erg}$
- Energy density: $u \sim 2 \times 10^6\text{erg cm}^{-3}$
- Pressure: $P_{rel} \sim 7 \times 10^{-7}\text{dyn cm}^{-2}$
- Synchrotron lifetime 1.6GHz: $\tau_{sync} \sim 2000\text{yr}$
- Equipartition field: $B_{eq} \sim 5\text{mG}$

Assuming that the relativistic pressure in the South Lobe is balanced by ram pressure:

$$P_{rel} \sim \rho v^2$$

We are not certain what ambient medium the jet is ramming into. The lack of 21-cm absorption or of maser amplification against the compact radio source shows that the molecular disk does not cover the central source. Ulvestad, Wrobel & Carilli (1999) estimate the emission measure of the free-free absorbing medium in front of the south lobe to be $10^7\text{cm}^{-6}\text{pc}$ and use the scale over which the spectral index varies to estimate the size of the absorbing cloud to be about 5pc. This yields an electron density in the medium

$$\langle n_e \rangle \sim 10^3\text{cm}^{-3}$$

Comparison of our 1.67GHz map with their 1.4GHz map shows a spectral index inversion which yields a consistent result for free-free absorption. If this represents the density in the shock ionized interaction region, then the column length may be much smaller resulting in a correspondingly higher electron density. This density would be, however, a factor of 4 higher than the density of the ambient medium. If we take as an upper limit $n \lesssim 10^4\text{cm}^{-3}$, this places a *lower* limit on the lobe-advance speed,

$$v_{adv} \gtrsim 2 \times 10^{-4}c$$

and thus an upper limit on the age of the recent outburst,

$$\tau_{rs} \lesssim 5 \times 10^5 \text{yr}$$

Considering the uncertainties in the above analysis, a comfortable age limit might be of the order of a million years. We have speculated (Smith *et al.* 1999) that this limit, combined with the suggested youth of the CSOs, implies that Mrk 231 is a young QSO, emerging from the shroud of dust along the lines of the Sanders *et al.* (1988) scenario. Of course, we do not know that this is the first AGN-related outburst. If the kpc-scale emission is, indeed, produced by a jet from the nucleus, then this suggests an earlier AGN event has occurred, probably early in the same $\sim 10^8$ year merger episode of which we are now witnessing the last stages.

If the advance speed in Mrk231 is as large as the speeds measured by Taylor *et al.* (2000), then the CSO in Mrk 231 has an age of the order of only 1000 yr. In this case the southern lobe movement since our original observations would be approaching a milliarcsecond and will be directly measurable in the near future.

Taylor *et al.* (1999) report detection of four candidate luminous radio supernovae between 0.2–0.5mJy in Mrk 231 within a 100 pc region of the central source. There is a faint unresolved source with flux density 0.5mJy near the position of their brightest RSN candidate “A” on our image taken just over two years earlier. Since the flux density is comparable over the two year interval, “A” appears unlikely to be an RSN and more likely to be related to the AGN core, a possibility noted by Taylor *et al.* (1999). We note, however, that the luminous RSN in Arp 220 exhibit longer decay times than do “normal” LRSN (Lonsdale *et al.* 2001) so that longer timelines are necessary to establish the nature of candidate “A” conclusively. We do not see sources near their candidates B, C or D; Taylor *et al.* note that these may be artifacts. Since the bulk of the starburst-related radio emission appears to be coming from the HI/molecular disk, we would expect RSN to be found in that region, as is the case with NGC 7469 (Colina *et al.* 2001).

3.3.2. OH Maser Emission in Mrk 231

The OH megamaser in Mrk 231 has a spectrum typical of the class (*e.g.* Staveley-Smith *et al.* 1987), with a velocity width of several hundred km/s. It is one of the most luminous OH megamasers known ($10^{2.9} L_{\odot}$), and was one of the first to be discovered (Baan 1985). As described above, Mrk 231 also exhibits strong, compact continuum emission, which we would expect to be amplified by any diffuse foreground OH masing screen, yielding bright

maser structures on VLBI scales; based on our picture of the geometry of the inner regions of Mrk 231, we might expect compact OH megamaser amplification spots against the northern radio continuum lobe, but not against the core and southern lobe, to which we apparently have a clear line of sight to the south of the inclined HI and molecular disk. We might also expect compact high-gain (apparently saturated) masers of the type discovered in Arp 220 (Lonsdale *et al.* 1998), IIZw35, and IRAS 17208–0014 (Diamond *et al.* 1999) for which no detectable background continuum source exists.

To our surprise, no such compact structures of either sort exist in Mrk 231, on scales significantly smaller than ~ 0.1 arcseconds. At the locations of the brightest continuum emission, upper limits on the maser amplification ratio S_{line}/S_{cont} are of order 0.05. At the location of the northern lobe, the lack of detectable compact maser emission gives an amplification ratio limit of order unity.

Our OH image of Mrk 231, integrated over the 1667MHz line, is shown in Figure 4. The diffuse OH emission we detect is poorly imaged due to the paucity of short baselines in our array, but based on the information thus gleaned, the location and extent of the emission is consistent with an origin in the molecular disk of material identified by Bryant & Scoville (1996), and is likely to be amplified radio continuum emission from this disk, emission which was imaged by Taylor *et al.* (1999). The OH emission in Mrk 231, which lacks any compact component, is thus consistent with the classical OH megamaser model for diffuse emission originally presented by Baan (1985).

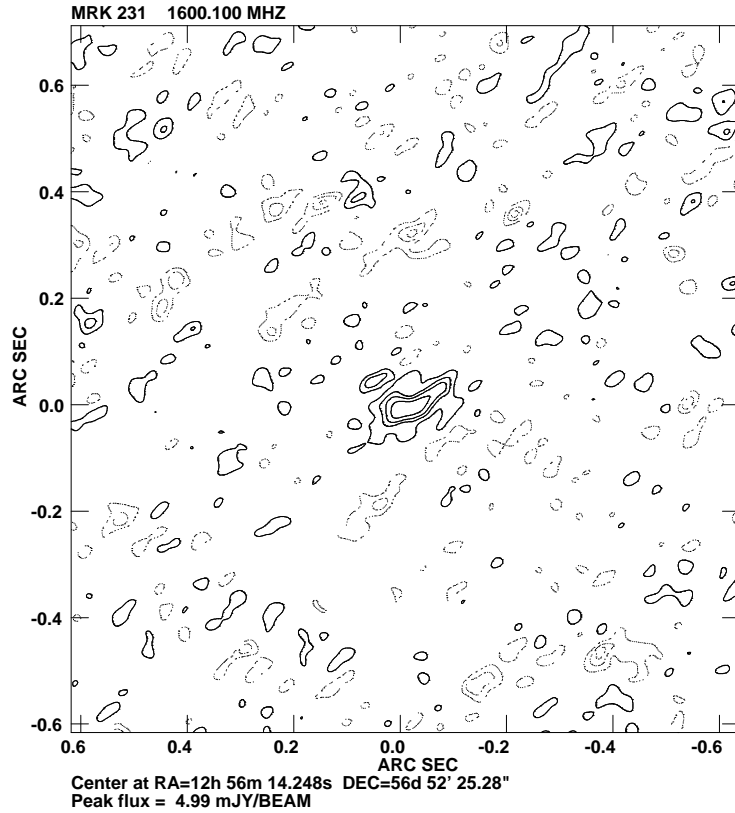


Fig. 4.— OH 1667MHz maser image of Mrk 231. Axes are the RA and DEC offsets from the continuum core center. This image was made by averaging all frequency channels with continuum-subtracted maser emission, discarding the longer baselines, and tapering the (u,v) data to improve angular resolution, thereby improving the surface brightness sensitivity relative to a full resolution image. Contours are -2.7, -1.9, -1.0, 1.0, 1.9, 2.7, 3.7 mJy.

4. Discussion

In each of the three galaxies our imaging results have demonstrated that the radio continuum on scales of ~ 100 pc is dominated by an AGN, not a starburst. Our VLBI imaging shows that the compact emission is characterized by well-defined ridgelines and high brightness yet spatially resolved components. The structure and flux densities of these VLBI components are not consistent with starburst-generated radio supernovae of the type found in Arp 220.

In all three cases, an unresolved AGN core has also been detected in the NIR and MIR, with upper limits comparable to the size of the AGN-dominated 18cm core structure.

Our direct measurements of the 18cm AGN-related core radio flux for these three objects are 38 ± 4 mJy for UGC 5101, 15 ± 1 mJy for NGC 7469 and 91 ± 9 mJy in Mrk 231. For UGC 5101 and NGC 7469 our measured values may be an underestimate of the total flux from the AGN due to flux on intermediate scales missed by our long baselines. For NGC 7469 a better estimate of the AGN flux is the 30 mJy detected in the compact source by MERLIN by Thean *et al.* (2001), which is twice as high as the 15 mJy detected by the longer baselines of our VLBA map.

4.1. The Circumnuclear Regions

We emphasize that, in addition to AGN activity, each LIG is characterized by an intense starburst in the central regions. However since we have clearly demonstrated that the inner 100pc or so is dominated at 18cm by the AGN in each case, the starburst is a circumnuclear one, and there must be an interface region between the two phenomena.

To investigate the relationship of the AGN and starburst in these three galaxies we have computed the “infrared-to-radio parameter” q , the ratio of infrared to radio 20cm flux density (CHYT), as a guide to the infrared emission expected from the starburst. q has been found to have a remarkably limited dispersion over 5 orders of magnitude in luminosity for star-forming regions and galaxies (Yun *et al.* 2001). Table 5 presents the results of this calculation.

As a first estimate for q for the starburst, q_{sb} , we assume that: 1) the VLBI emission, S_{vlbi} (column 9, corrected by 8% from 18cm to 20cm assuming a spectral index of 0.7), is produced by the AGN, 2) more extended emission, $S_{vla} - S_{vlbi}$ (column 8 – column 9) is produced by the circumnuclear starburst, 3) the unresolved nuclear mid-infrared ($12\mu\text{m}$) component is produced by the AGN, while 4) extended mid-infrared emission is starburst

related. Assuming that the mid-infrared component ratios reflect those in the far-infrared we obtain the Starburst fraction (column 5) and AGN fraction (column 6) and the Starburst Luminosity (column 3) and AGN Luminosity (column 4). Since we expect the AGN component to be warmer in the infrared, this represents a lower limit to the Starburst fraction and Luminosity. It is worth noting that Farrah *et al.* (2003) obtain a very similar Starburst fraction (60%) for Mrk 231 based upon SED modeling.

The resulting values of q_{sb} are given in column 10 of Table 5. The values for all three galaxies are significantly low, *i.e.* relatively radio-loud, compared to a canonical average value of 2.34 (CHYT) for star-forming galaxies. This may indicate that we have underestimated the fraction of the bolometric luminosity arising in the starburst vs the AGN; however, it would require essentially *all* of the measured IR luminosity of NGC 7469 and Mrk 231 to force q_{sb} to 2.34, and for UGC 5101 q_{sb} would still be 50% low: 2.17. Such a solution is implausible given the MIR core luminosities detected directly in each of the 3 LIGs (Soifer *et al.* 2000, 2003; Miles, *et al.* 1996).

One obvious way to reconcile the low q_{sb} values is to assume that some of the radio emission on larger size scales, which we have attributed to the starburst, in fact arises ultimately from the AGN instead, either from unrecognized jet structure or energy pumped into the dense ISM from the central AGN in a more spatially distributed manner which is unrecognized in the VLA maps. To follow this argument to a logical limit we derived the total radio flux that must be attributed to the AGN instead of the starburst in order to raise q_{sb} to 2.34; the result is given in column 11 of Table 5. We find we would have to multiply the VLBI-scale detected flux of UGC 5101 by 2.3 to 93 mJy to force $q_{sb} = 2.34$. The MERLIN-detected flux of NGC 7469 would have to be tripled to 113 mJy, while the core and lobe emission of 98 mJy of Mrk 231 would need to be increased by a factor of 1.4 to 140 mJy (column 11 of Table 5).

We conclude that if we expect a nominal q value of 2.34 in the circumnuclear starbursts in these three galaxies, then the radio flux due to the AGN is ~ 1.5 to 3 times larger than that detected on long baselines in the compact cores of these sources. A similar analysis by Roy *et al.* (1998) and Corbett *et al.* (2002) for two different samples of AGN with compact radio cores, has resulted in similar conclusion: they find evidence for radio structures associated with the compact AGN radio core source which extend tens to hundreds of pc around the core.

Table 5. The Starburst Infrared-to-Radio Ratio, q_{sb}^\dagger

Galaxy	$\log L_{IR}$ (L_\odot)	$\log L_{SB}$ (L_\odot)	$\log L_{AGN}$ (L_\odot)	Starburst fraction	AGN fraction	q_{tot}	S_{vla} (mJy)	S_{vlbi} (mJy)	q_{sb}	S_{AGN} (mJy)
(1)	(2)	(3)	(4)	(5)	(6)	(7)	(8)	(9)	(10)	(11)
UGC 5101	11.96	11.81	11.44	0.7	0.3	2.06	146	41.2	2.05	93
NGC 7469	11.60	11.30	11.30	0.5	0.5	2.24	183	32.5	2.02	113
Mrk 231	12.51	12.29	12.11	0.6	0.4	2.19	240	98.6	2.20	140

$^\dagger q_{tot}$ and L_{IR} are revised slightly from the values given by Smith, Lonsdale & Lonsdale (1998) because the IRAS fluxes of these galaxies have been revised in a new study by Sanders *et al.* (2003).

4.2. AGN Radio Core Powers and a Comparison to Radio Quiet QSOs

Lonsdale, Smith & Lonsdale (1995) showed that radio quiet PG QSOs follow a relationship between the core radio power and bolometric luminosity, and that ULIRGs with VLBI-scale emission follow a similar relation with higher scatter. This is illustrated in Figure 5, where we plot PG QSOs with $z < 0.6$, and the new core power estimated for the 3 LIGs, corrected to 20 cm assuming a power law slope of 0.7, and the assumed AGN bolometric luminosities given in Table 5. Compared to the median radio quiet PG QSO relation (the lower sequence of points in Figure 5; the upper sequence of points are radio-loud PG QSOs), all three LIGs have over-luminous radio cores, by factors of about 14, 8, and 10 for UGC 5101, NGC 7469 and Mrk 231 respectively. If we plot the revised AGN-related radio fluxes resulting from the q analysis above (column 11 of Table 5; small closed symbols), these LIGs will be even more over-luminous in the radio — these appear to be radio-loud QSOs.

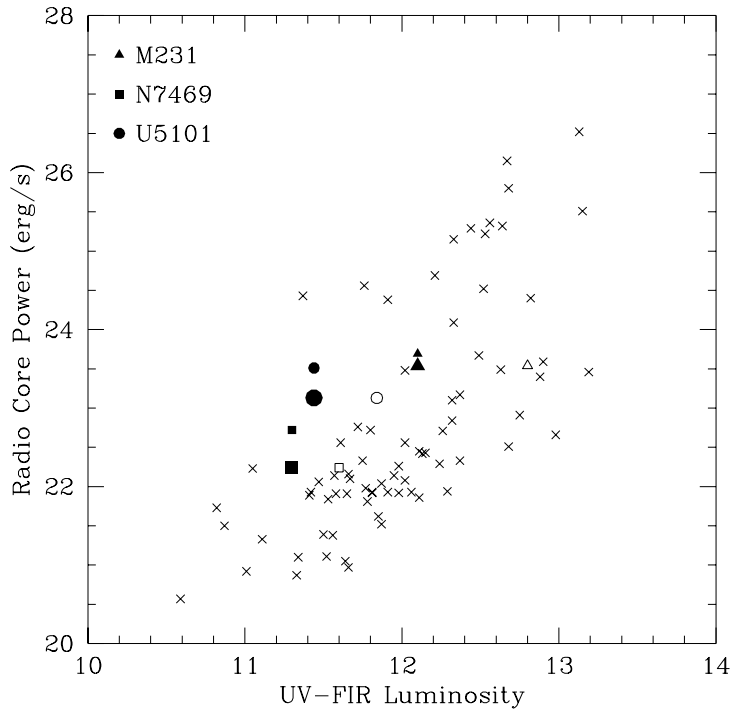


Fig. 5.— Integrated UV to FIR luminosity *vs* radio core power at 21cm for the three LIGs compared to PG QSOs (Lonsdale, Smith & Lonsdale 1995). Each AGN is plotted three times; the large filled symbols show the core radio power corresponding to the measured flux which we attribute to the AGN cores, 38/15/88 mJy for UGC 5101/NGC 7469/Mrk 231, respectively, and assuming the AGN luminosity fraction given in column 4 of Table 5. The small filled symbols represent the core radio power in Column 11 of Table 5. The small open symbols represent the maximum possible AGN UV-FIR luminosity in the extreme case that the contribution of the starburst is negligible, and that some flux has been missed altogether due to beaming (§4.3). All three AGN appear to be over-luminous in the radio compared to PG QSOs, except possibly Mkn 231 under extreme assumptions.

The radio loudness would be reduced if the bolometric luminosity of the AGN has been under-estimated, however there is not enough *total* measured UV-FIR luminosity (Table 5, column 2) to shift these LIGs to the median PG QSO relation. It is possible some AGN luminosity has been missed altogether due to absorption/beaming (small open symbols; see section 4.3 for analysis and discussion), which might make Mrk 231 consistent with the PG QSO relation, but probably not the other two LIGs.

Are these three objects in fact radio loud AGN in the classic sense of high power output from the nucleus in the form of jets? It is thought that radio power is a function of black hole mass and accretion rate (Lacy *et al.* 2001; Laor 2000) and we certainly might expect accretion rate to be high in these dust and gas rich objects. Or are they unusually luminous in the radio because a low power AGN radio source is running into unusually dense ISM in the circumnuclear starburst?

4.3. Constraining the Extinction and the Core AGN Luminosity Using NIR and MIR Data

An unresolved nuclear point source has been detected in each of the three LIGs studied here with either HST or AO imaging in the near-IR J, H and K bands and also in the MIR (see Section 1 for details). This emission is assumed to arise in the central core regions of the AGN itself; extensive studies of NIR and MIR SEDs of Seyfert galaxies and QSOs indicates that the MIR emission is most likely due to a warm, dusty, molecular torus, and the NIR emission can arise either from the inner hot regions of the torus from dust near 1000K, and/or from dust entrained in outflow cones perpendicular to the accretion disk of the AGN, perhaps near the location of the narrow line clouds (Efstathiou & Rowan-Robinson 1995; Efstathiou, Hough & Young 1995; Granato, Danese & Franceschini 1997; Nenkova, Ivezić & Elitzur 2002).

The MIR luminosity of Seyfert galaxies and quasars is potentially a good indicator of both the blue luminosity and the X-ray luminosity, for AGN with modest N_H columns, and presumably also the bolometric luminosity (Polletta *et al.* 2000; Haas *et al.* 2000; Alonso-Herrero *et al.* 2001). The near-IR luminosity is less well correlated with the X-ray luminosity than is the MIR luminosity, probably due to a combination of increased effects of extinction, but is still a useful diagnostic.

The analysis of the extinction to these regions is a highly complex topic. It is well known that simple comparisons of E_{B-V} from optical line ratios to N_H derived from X-ray absorption measurements often do not reflect a self-consistent extinction law resembling

that of the Galaxy. Maiolino *et al.* (2001) argue that this indicates unusual dust grain composition in the core regions of AGN, rather than a different line-of-sight path for the X-rays compared with the BLR or other explanations.

A detailed analysis of this issue is beyond the scope of this paper. Here we address the specifics of the NIR and MIR emission and extinction for our 3 LIGs, insofar as it can help to constrain the underlying AGN luminosity.

The PG QSOs investigated by Lonsdale, Smith & Lonsdale (1995) display a remarkably uniform distribution of JHK colors. This is illustrated in the tight and parallel relations between J, H and K absolute magnitudes as a function of integrated UV-FIR luminosity in Figure 6, where we have restricted the PG sample to objects with $z < 0.2$ so that the NIR part of the rest frame spectrum is being sampled. This behavior allows a meaningful comparison to the LIG colors, even though the path and extinction law of any extinction to the LIG AGN cores may not be well understood.

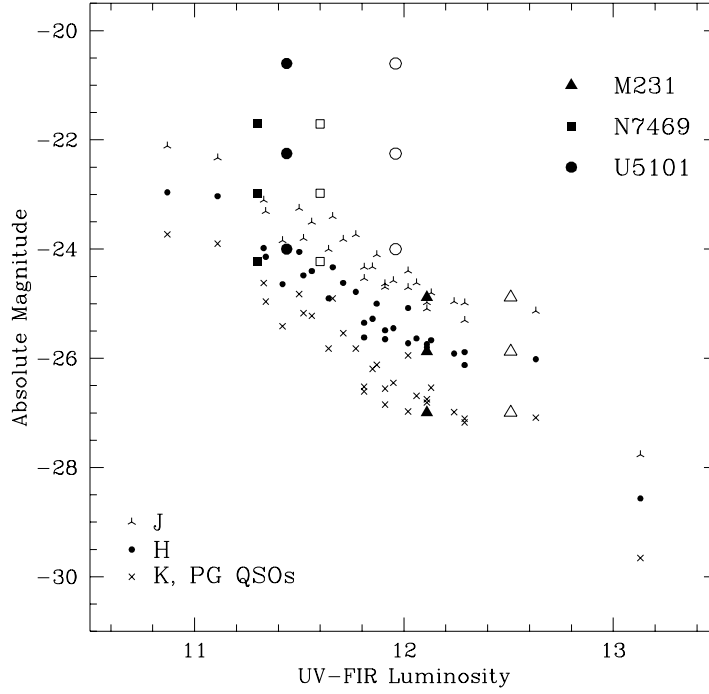


Fig. 6.— Absolute J, H and K core magnitudes *vs* integrated UV to FIR luminosity for the three LIGs compared to optically-selected QSOs (“PG QSOs”) from the Palomar-Green survey (Neugebauer *et al.* 1987) (small symbols, different for each band). The 3 types of large symbol are different for each LIG but the same for each band; J is always the upper of the three symbols and K the lower. The filled symbols reflect the AGN luminosity fraction in column 4 of Table 5 and the open symbols reflect the total UV-FIR luminosity. The QSOs form well behaved sequences which allows an analysis of the LIG colors. Mrk 231’s colors resemble those of the QSOs so it is probably relatively unreddened in the NIR or has grey extinction. Fitting to the QSO sequence (filled triangles) produces an estimate of the QSO UV-FIR luminosity for this galaxy, reported in column 4 of Table 5. The other two LIGs show evidence of extinction in their NIR colors.

In Figure 6 we have plotted the core J, H and K sources of each LIG twice: once against the total near- to far-IR luminosity of the object (Sanders *et al.* 2003), and once with the AGN luminosity fraction listed in Table 5. There is a quantitative difference in the location of Mrk 231 and the other two LIGs in this figure: Mrk 231 displays the same colors as the PG QSOs. This indicates that it has the same SED shape as these relatively unreddened QSOs, and is therefore probably itself essentially unreddened in the NIR. For a Galactic extinction law, the reddening measured in the optical, $A_V \sim 2.0$ mag, corresponds to $A_K \sim 0.2$ mag, which is unmeasurable against the dispersion of the PG colors in Figure 6. The other two LIGs show larger relative separations between the bands, and moreover $[\text{mag}_{LIG} - \text{mag}_{QSO}]$ at the luminosity of the LIG increases from K to H to J, in the sense expected for the effect of reddening. These two LIGs therefore probably display reddening in the NIR to the nuclear point source, that is to the core of the AGN. Note, however, that an analysis of the MIR core flux in section 4.3 may amend this conclusion.

If the nuclear point source in Mrk 231 is unreddened in the NIR then it must also suffer little extinction unless the extinction is grey. We can therefore use the measured NIR absolute magnitudes to fit Mrk 231 horizontally to the PG QSO relations, thereby estimating the true luminosity of the AGN in this source, as given in Table 5: $\log L = 12.11$ (L_\odot) with AGN luminosity fraction 40%. Consequently the left-most points representing Mrk 231 in Figure 5 fit nicely onto the QSO sequences because they have been forced to fit.

For UGC 5101 and NGC 7469 we have attempted fits using a Galactic extinction law (Mathis 1990). This analysis should only be considered indicative of luminosities and extinctions for several reasons. First, the intrinsic uncertainty in the extinction due to the dispersion in the QSO relations is large: ~ 0.7 mag. Also, we cannot rule out (a) a different reddening law from Galactic; (b) scattering which could blue the colors (*eg.* NGC 7469); or (c) emission from hot dust which could redden the $[H - K]$ color, as suggested by Scoville *et al.* (2000) for UGC 5101. Furthermore we may have underestimated the bolometric luminosities of either the PG QSOs or the LIGs by excluding X-ray emission, therefore introducing uncertainty in the horizontal separation of the LIGs from the QSOs.

For UGC 5101, with an assumed AGN luminosity of 11.44, we find a consistent fit across the three bands with $A_V = 8.9 \pm 1.0$. For NGC 7469, with an assumed AGN luminosity of 11.3, however, the apparent extinction required to correct the J, H and K bands to the PG QSO sequence is $A_V = 3.2, 3.9$ and 5.9 respectively, which displays inconsistency in the extinction law. The discrepancy from the Galactic extinction law is in the sense of the de-reddened LIG colors being too blue. If we take a smaller value for the AGN luminosity the extinction correction decreases in size and shifts to better agreement with the Galactic law; an optimum value occurs at about $L_{AGN} = 11.2$ and $A_V = 1.9$.

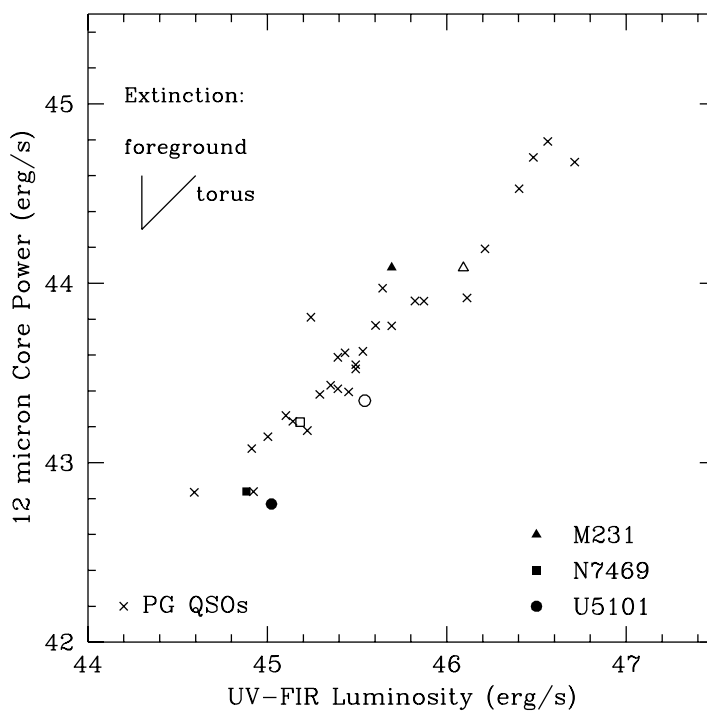


Fig. 7.— 12 μm core power for the three LIGs *vs* integrated UV to FIR luminosity compared to PG QSOs (Neugebauer *et al.* 1987). Filled symbols reflect the AGN luminosity fraction in Table 5 column 4 while open symbols reflect the total observed UV-FIR luminosity. The approximate effect of a factor of two extinction is indicated in the upper left-hand corner, depending upon dust geometry. UGC 5101 appears somewhat under-luminous compared to radio-quiet QSOs and may suffer significant extinction. Mrk 231 appears slightly over-luminous.

Finally in Figure 7 we show the relation between integrated UV-FIR luminosity (Lonsdale, Smith & Lonsdale 1995) and core $12\mu\text{m}$ power. For the PG QSOs we take the total IRAS flux as reported by Sanders *et al.* (1989), limiting the sample to $z < 0.4$ so that the $12\mu\text{m}$ filter does not shift shortward of the $7\mu\text{m}$ MIR bump. For the LIGs we plot the $< 100\text{pc}$ -scale $12\mu\text{m}$ core source (solid symbols) (Soifer *et al.* 2000, 2003; Miles, *et al.* 1996), taking as the AGN power the luminosity given in Table 5 column 4. Also shown (open symbols) are total IRAS $12\mu\text{m}$ powers vs total luminosity (column 2 of Table 5). The PG QSO power could be overestimated if there is substantial star formation within the large IRAS beam (Haas 2001). The PG QSOs show a very tight relation in this figure, with $12\mu\text{m}$ power $\sim 1\%$ of total power (neglecting the X-ray range).

The effects of a factor of 2 extinction in Figure 7 are shown. Since the source of the MIR emission is thought to be a dusty torus which can become optically thick in the MIR, a detailed radiative transfer model is required to describe the source. Silicate absorption features are indicative of overall extinction, however the equivalent width of such features depends not only on the intrinsic equatorial optical depth of the torus, but on the inclination to the line of sight, the torus height, and the dust temperature. Inclination is the biggest overall factor in MIR extinction, with edge-on disks being strongly attenuated in observed luminosity. The absorbed MIR luminosity of such an inclined torus is not necessarily detected at longer IR wavelengths after absorption and re-emission from more distant, cooler dust grains, because the torus does not emit isotropically.

In Figure 7 we see that the uncorrected $12\mu\text{m}$ core power of UGC 5101 is low by a factor of 2–2.5 compared to the PG QSOs (though the QSO relation is not strongly defined in this luminosity range) and that UGC 5101 is more under-luminous compared to the QSOs than the other two LIGs. This could either mean that there is considerable extinction at $12\mu\text{m}$ or that the UV-FIR AGN luminosity has been over-estimated. We favor the first interpretation because in large aperture ISO spectra, UGC 5101 shows the deepest water ice absorption at $6.0\mu\text{m}$ among the SEDs reported by Spoon *et al.* (2002), coupled with a very strong silicate absorption and PAH emission. Also, the core JHK colors are significantly redder than for NGC 7469 and Mrk 231, as shown in Figure 6. Thus a consistent picture arises in which the AGN core of UGC 5101 is more heavily absorbed throughout the NIR and MIR than the other 2 LIGs, and in which the $12\mu\text{m}$ core luminosity in Figure 7 (filled circle) is an underestimate of the AGN MIR luminosity.

Although the $12\mu\text{m}$ AGN luminosity is underestimated in Figure 7, the *total* luminosity of the UGC 5101 AGN (horizontal axis) is not necessarily affected since it is an independently inferred parameter. However the bolometric luminosity of the entire galaxy may have been underestimated due to MIR extinction, depending on where the extinction occurs, and this

would affect the analysis of Section 4.1 and the inferred total AGN luminosity. Specifically, if the extinction occurs in front of the torus in the starburst medium, the absorbed MIR flux will have been accounted for in the total far-infrared emission detected by IRAS (open circle in Figure 7) and the Section 4.1 analysis is unaffected. However, if the observed MIR extinction occurs within a torus inclined partly into our line-of-sight, it is possible the some of the missed flux is beamed out of our line-of-sight altogether. In that case the total galaxy luminosity is underestimated by IRAS (column 2 of Table 5), the starburst vs AGN luminosity fraction would decrease in the analysis of Section 4.1 (columns 5 and 6), and the total AGN luminosity of column 4 would increase. Thus both data points in Figure 7 would shift up and to the right.

NGC 7469 is more consistent with the QSO relation in Figure 7, though perhaps a little under-luminous. Alonso-Herrero *et al.* (2001) have modelled the NIR and MIR emission of NGC 7469 with the torus models of Efstathiou & Rowan-Robinson (1995), finding that the flat SED requires a viewing angle $< 30^\circ$, *ie.* close to face on. In that case little of the MIR emission would be lost to extinction (see Figure 9 of Alonso-Herrero *et al.* (2001)). This is generally consistent with the small, but detectable, NIR extinction inferred from the nuclear NIR colors (Figure 6).

In contrast, for Mrk 231 the core $12\mu\text{m}$ power is somewhat over-luminous unless we have underestimated the bolometric AGN luminosity by a factor of about 2.5. It's unlikely that this missing luminosity is represented by the total UV-FIR measurement (open triangle) because that would leave nothing over for the starburst, therefore this missing luminosity would need to be attributed to power missed by the IRAS measurements, *eg.* high frequency UV-X-ray flux beamed away from the line-of-sight. There is indeed evidence for a very high X-ray absorbing column to the core of Mrk 231 (Gallagher *et al.* 2002), which is probably sufficient to hide a nuclear hard X-ray source of $\gtrsim 10^{44}$ erg s $^{-1}$, as implied by the MIR power by Figure 17 of Alonso-Herrero *et al.* (2001).

Moreover, the MIR SED of Mrk 231 is probably significantly absorbed, exacerbating the apparent underestimation of the core AGN power deduced from Figure 7. Mrk 231 has a very similar 2–20 μm SED shape to NGC 7469 (Spoon *et al.* 2002; Soifer *et al.* 2000), except for the significant silicate absorption feature. To reproduce such a feature there could be foreground extinction by the starburst medium, or the torus could be significantly more inclined to the line-of-sight, or of higher equatorial optical depth, in which case the MIR luminosity of the torus that we observe may underestimate the face-on luminosity by a factor of 2 or significantly more. Such a result would seem at face value to be inconsistent with the conclusion from Figure 6 that the NIR core source is relatively unreddened. However such a flat $1 < \lambda < 7\mu\text{m}$ SED (Soifer *et al.* 2000) can instead be explained as additional warm

dust emission from the AGN cone, as modelled for NGC 1068 (Efstathiou, Hough & Young 1995).

In summary, there is evidence from the NIR and MIR observations that the AGN power of Mrk 231 may be underestimated in Table 5 (column 4) by a (highly uncertain) factor of about 5. Similarly the AGN power for UGC 5101 may be underestimated by a factor of two and overestimated by a similar factor for NGC 7469 though a factor of two is well within the uncertainty of this analysis. This AGN power may be unaccounted for in the total galaxy luminosities listed in column 2 also; this is almost certainly the case for Mrk 231. This unaccounted AGN power in Mrk 231 may be enough to bring it into line with the most luminous radio quiet QSOs in Figure 5 (open symbols), but UGC 5101 and NGC 7469 remain radio-loud in that plot. Detailed hard X-ray spectroscopy and modelling will be required to resolve this question.

4.4. The OH Megamaser

Among OH megamaser sources which have been studied at milliarcsecond resolutions, Mrk 231 is currently unique in the lack of compact structures. Well-studied sources such as Arp 220 (Lonsdale *et al.* 1998) and III Zw 35 (Diamond *et al.* 1999) have compact maser structures which account for many tens of percent of the total OH luminosity. Darling and Giovanelli (2002a) report temporal variability in one distant OH megamaser, and cite further evidence for widespread saturated (and thus compact) maser emission in $z > 0.1$ megamaser galaxies (Darling & Giovanelli 2002b).

Clues to this unique lack of compact OH megamaser emission in Mrk 231 may come from understanding other ways in which Mrk 231 is unusual. The most obvious one is that the AGN core is relatively unobscured in the optical-NIR, suggesting that it lies further along the presumed starburst-AGN evolutionary track. We speculate that as the AGN injected copious quantities of both mechanical and radiative energy into the original dense circumnuclear shroud, as evidenced by the BAL wind and the radio jets, much of the cool molecular environment most conducive to the formation of compact masers was destroyed. This destruction is likely to have been complete in the AGN outflow cones. Mrk 231 may be a rare transition object in which the compact masers have been destroyed, but some diffuse maser clouds in the outer disk have so far survived.

However a strong circumnuclear starburst remains, which is extremely luminous in its own right and which might be expected to contain compact masers like those found in the Arp 220 starburst region. This region, roughly perpendicular to the AGN outflow axis, and

of ~ 400 pc dimension, has not been cleared out by the AGN; indeed a dense optically thick molecular torus is thought to still exist, along with a high column, low ionization BAL wind at smaller radii. Thus the lack of detectable OH emission coincident with the northern continuum lobe is particularly surprising, since the starburst disk geometry proposed by other workers suggests that part of the disk should lie in front of that lobe, which exhibits strong free-free absorption.

One factor which might influence the existence of compact maser clouds is the overall density in the Mrk 231 starburst. Unlike Arp 220, it extends about ~ 400 pc in diameter, and thus has a star-formation surface density of $2 \times 10^{-4} M_{\odot} \text{yr}^{-1} \text{pc}^{-2}$, a factor of approximately 16 less than Arp 220. These lower density conditions in the later stages of a starburst may inhibit the formation or pumping of compact maser clouds. Additionally, the lack of amplified continuum VLBI structures may be explained by the likelihood that the cooler, outer regions of the disk will harbor most of the OH maser clouds. These outer regions may lie, in projection, to the north of all the continuum VLBI-scale structure.

Thanks to Chris Carilli for providing us with a digital 1.4GHz image of Mrk 231 for comparison with our data and to Tom Soifer and Jamie Bock for discussing their mid-infrared imaging of NGC 7469. CJL and HES thank the NRAO VLA AOC for hospitality and assistance. HES wishes to express gratitude to IPAC for providing continued support. IPAC/JPL is supported by NASA. Haystack is supported by the NSF via NEROC. Support of this project at UCSD has been provided by the NSF. The National Radio Astronomy Observatory is a facility of the NSF operated under cooperative agreement by Associated Universities, Inc. This research has benefitted from the NASA/IPAC Extragalactic Database, which is operated by JPL/Caltech under contract with NASA.

REFERENCES

- Adams, T., & Weedman, D. 1972, *ApJ*, **173**, L109.
- Alonso-Herrero, A., Quillen, A., Simpson, C., Efstathiou, A. & Ward, M. 2001, *AJ*, **121**, 1369.
- Baan, W. 1985, *Nature*, **315**, 26.
- Baum, S., O’Dea, C., Dallacassa, D., de Bruyn, A. & Pedlar, A. 1993, *ApJ*, **419**, 553.
- Boksenberg, A., Carswell, R. F., Allen, D., Fosbury, R., Penston, M. & Sargent, W. 1977, *MNRAS*, **178**, 451.

- Boroson, T., Meyers, K., Morris, S., & Persson, S. E. 1991, ApJ, **370**, L19.
- Bryant, P. & Scoville, N. Z. 1996, ApJ, **457**, 678.
- Carilli, C. L., Wrobel, J. M., & Ulvestad, J. S. 1998, AJ, **115**, 928.
- Colina, L., Alberdi, A., Torelles, J. & Wilson, A. 2001, ApJ, **553**, L19.
- Condon, J. J., Huang, Z.-P., Yin, Q. F., & Thuan, T. X. 1991, ApJ, **378**, 65 (CHYT).
- Conway, R. G., Birch, P., Davis, R., Jones, L., Kerr, A., Stannard, D., 1983, MNRAS, **202**, 813.
- Corbett, E. A., et al. 2002, ApJ, **564**, 650.
- Dahari, O. 1985, ApJS, **57**, 643.
- Darling, J. & Giovanelli, R. 2002a, ApJ, **569**, L87.
- Darling, J. & Giovanelli, R. 2002b, AJ, **124**, 100.
- Dermer, C., Bland-Hawthorn, J. Chiang, J., & McNaron-Brown, K. 1997, ApJ, **484**, L121.
- De Rosa, A., Fabian, A. C. & Piro, L. 2002, MNRAS, **334**, L21.
- Diamond, P. J., Lonsdale, C. J., Smith, H. E., & Lonsdale, C. J. 1999, ApJ, **511**, 178.
- Efstathiou, A., & Rowan-Robinson, M. 1995, MNRAS, **273**, 649.
- Efstathiou, A., Hough, J. H. & Young, S. 1995, MNRAS, **277**, 1134.
- Farrah, D., Efstathiou, A., Alfonso, J., Rowan-Robinson, M., Fox, M., & Clements, D. 2003, MNRAS, *in press*.
- Forster, K., Rich, M. & McCarthy, J. 1995, ApJ, **450**, 74.
- Gallagher, S. C., Brandt, W., Sambruna, R., Mathur, S. & Yamasaki, N. 1999, ApJ, **519**, 549.
- Gallagher, S. C., Brandt, W., Chartas, G., Garmire, G. & Sambruna, R. 2002, ApJ, **569**, 655.
- Granato, G. L., Danese, L., & Franceschini, A. 1997, ApJ, **486**, 147.
- Hamilton, D. & Keel, W. 1987, ApJ, **321**, 211.

- Haas, M. 2001, *New Astronomy Reviews*, **45**, 617.
- Haas, M. *et al.* 2000, *A&A*, **354**, 453.
- Henstock, D. *et al.* 1995, *ApJS*, **100**, 1.
- Lacy, M., Laurent-Muehleisen, S. A., Ridgway, S. E., Becker, R. H. & White, R. L. 2001, *ApJ*, **551**, L17.
- Lai, O., Rouan, D., Rigaut, F., Arsenault, R., & Gendron, E.
- Laor, A. 2000, *ApJ***543**, L111.
- Lipari, S., Colina, L. & Macheto, F. 1994, *ApJ*, **427**, 174.
- Lonsdale, C. J., Diamond, P. J., Lonsdale, C. J., & Smith, H. E. 2001, in *Galaxies and their Constituents at the Highest Angular Resolutions; IAU Symposium 205*, ed R. T. Schilizzi, p. 386.
- Lonsdale, C. J., Diamond, P. J., Smith, H. E., & Lonsdale, C. J. 1998, *ApJ*, **493**, L13.
- Lonsdale, C. J., Smith, H. E., & Lonsdale, C. J. 1993, *ApJ*, **405**, L9 (Paper I).
- Lonsdale, C. J., Smith, H. E., & Lonsdale, C. J. 1995, *ApJ*, **438**, 632.
- McCutcheon, W. & Gregory, P. 1978, *AJ*, **83**, 566.
- Maiolino, R. *et al.* 2001, *A&A*, **365**, 28.
- Maloney, P. R. & Reynolds, C. S. 2000, *ApJ*, **545** 23.
- Mathis, J., 1990, *ARA&A*, **28**, 37.
- Mauder, W., Weigelt, G., Appenzeller, I. & Wagner, S. 1994, *A&A*, **285**, 44.
- Miles, Houck, J. & Hayward, T. 1994, *ApJ*, **425**, L37.
- Miles, Ashby, M., Hayward, T. & Houck, J. 1996, *ApJ*, **465**, 191.
- Murray, N., Chiang, J., Grossman, S. A., & Voit, G. M. 1995, *ApJ*, **451**, 498.
- Nandra, K. *et al.* 2000, *ApJ*, **544**, 743.
- Nenkova, M., Ivezić, Z., & Elitzur, M. 2002, *ApJ*, **570**, L9.

- Neugebauer, G., Green, R. F., Matthews, K., Schmidt, M., Soifer, B. T., & Bennett, J. 1987, *ApJS*, **63**, 615.
- Pearson, T. P., & Readhead, A. C. S. 1988, *ApJ*.
- Perry, J. J. & Dyson, J. E. 1985, *MNRAS*, **213** 665.
- Peterson, B. M. & Wandel, A. 2000, *ApJ*, **540**, L13.
- Politidis, A. *et al.* 1995, *ApJS*, **98**, 1.
- Polletta, M., Courvoisier, T. J.-L., Hooper, E. J., & Wilkes, B. J. 2000, *A&A*, bf 362, 75.
- Quillen, A. C. *et al.* 2001, *ApJ*, **129**, 129.
- Readhead, A. C. S., Taylor, G., Xu, W., Pearson, T., Wilkinson, P., & Polatidis, A. 1996, *ApJ*, **460**, 612.
- Rigopoulou, D., Lawrence, A. & Rowan-Robinson, M. 1996, *MNRAS*, **278**, 1049
- Roy, A. L., Norris, R. P., Kesteven, M. J., Troup, E. R., & Reynolds, J. E. 1994, *ApJ*, **432**, 496
- Rudy, R., Foltz, C. & Stocke, J. 1985, *ApJ*, **288**, 531.
- Sanders, D., *et al.* 2003, *ApJ*, in press.
- Sanders, D. B. & Mirabel, I. F. 1996, *ARA&A*, **34**, 749.
- Sanders, D. B., Soifer, B. T., Elias, J., Madore, B., Mathews, K., Neugebauer, G., & Scoville, N. 1988, *ApJ*, **325**, 74.
- Sanders, D. B., Phinney, E. S., Neugebauer, G., Soifer, B. T., & Mathews, K., 1989, *ApJ*, **347**, 29.
- Sanders, D. B., Scoville, N. Z. & Soifer, B. T., 1991, *ApJ*, **370**, 158.
- Scoville, N. Z. & Norman, C. 1989, *ApJ*, **332**, 163.
- Scoville, N. Z., Yun, M. & Bryant, P. 1997, *ApJ*, **484**, 702.
- Scoville, N. Z., *et al.* 2000. *AJ*, **119**, 991.
- Seyfert, C. 1943, *ApJ*, **97**, 28.
- Smith, H. E., Lonsdale, C.J., & Lonsdale, C. J. 1998, *ApJ*, **492**, 137 (Paper II).

- Smith, H. E., Lonsdale, C.J., Lonsdale, C. J. & Diamond, P. J. 1998, ApJ, **493**, L17.
- Smith, H. E., Jones, B., Puetter, R. C., Stein, W. A., Wang, M., & Campbell, R. 1998, BAAS, **29**, 1331.
- Smith, H. E., Lonsdale, C.J., Lonsdale, C. J. & Diamond, P. J. 1999, Ap&SS, **266**, 125.
- Smith, P., Schmidt, G., Allen, R., & Angel, J. R. P. 1995, ApJ, **444**, 146.
- Soifer, B. T. *et al.* 2000, AJ, **119** 509.
- Soifer, B. T. *et al.* 2003, in preparation.
- Solomon, P., Downes, D., Radford, S., & Barrett, J. 1997, ApJ, **438**, 144.
- Spoon, H., Keane, J., Tielens, A., Lutz, D., Moorwood, A., & Laurent, O. 2002, A&A, **385**, 1022.
- Staveley-Smith, L., Cohen, R., Chapman, J., Pointon, L., & Unger, S. 1987, MNRAS, **226**, 689.
- Surace, J., Sanders, D., Vacca, W., Veilleux, S., & Mazarella, J. 1998, ApJ, **492**, 116.
- Taylor, G. B., Silver, C. S., Ulvestad, J. S., & Carilli, C. L. 1999, ApJ, **519**, 185.
- Taylor, G. B., Marr, J., Pearson, T., & Readhead, A. 2000, ApJ, **541**, 112.
- Terlevich, R. & Melnick, J. 1985, MNRAS, **213**, 831.
- Thean, A.H. ., Gillibrand, T. I., Pedlar, A. & Kukula, M. J. 2001, MNRAS, **327**, 369.
- Tran, Q. D. *et al.* 2001, ApJ, **552**, 527.
- Ulvestad, J. S., Wrobel, J. M. & Carilli, C. L. 1999, ApJ, **516**, 127.
- Wilkinson, P., Polatidis, A., Readhead, A., Xu, W., & Pearson, T. 1994, ApJ, **432**, L87.
- Wilson, A., Baldwin, J., Sze-Dung, S., & Wright, A. 1991, ApJ, **310**, 121.
- Yun, M., Reddy, N. & Condon, J. 2001, ApJ, **554**, 803.